INTERNATIONAL JOURNAL OF
NUMERICAL ANALYSIS AND MODELING, *SERIES B*
Volume 1, Number 1, Pages 1–24

BIFURCATION AND SENSITIVITY ANALYSIS OF IMMUNITY DURATION IN AN EPIDEMIC MODEL

NICHOLAS PIAZZA AND HAO WANG

(Communicated by Yau Shu Wong)

Abstract. Most disease transmission models assume no immunity or permanent immunity for simplicity, however, hosts have temporary immunity for most diseases. In this note we find that the immunity duration is actually the most sensitive parameter for dynamics of disease transmission. We provide numerical schemes to sketch Hopf bifurcations (forward or backward), sensitivity surfaces, periodicity diagrams (one dimensional or two dimensional parameter space) for a disease transmission model with immunity delay. The methods introduced here can be easily modified for a specific disease transmission model. We also test how different incidence functions change dynamics via bifurcation diagrams.

Key words. immunity duration, bifurcation, sensitivity, SIR, disease transmission.

1. Introduction

Modeling the dynamics of infectious diseases has become a topic of much interest in recent years. Such efforts are useful in disease control and in the prevention of outbreaks [1, 3]. Many types of infectious agents exist, all of which have their own unique set of behaviors. We can typically categorize infectious agents as one of the following: viral pathogens, bacterial pathogens, or parasitoids. Examples of such are as follows:

Viral	**Bacterial**	**Parasitic**
HPV	E. Coli	Malaria
AIDS	Typhus	Scabies
SARS	Cholera	
Mumps	Tetanus	
Measles	Syphilis	
Influenza	Botulism	
Viral Hepatitis	Pink Eye	
Mononucleosis	Gonorrhoea	
Common Cold	Salmonellosis	
Yellow fever	Lyme Disease	
Small Pox	Meningitis	
Rubella	Typhoid	
Herpes	Anthrax	
Ebola		

Different infectious agents exhibit different traits and thus different dynamics arise. Parameters that depend on the specific agent include the transmission rate, the recovery rate, and the subsequent immunity duration corresponding to the specific infection. Parameters that are independent of the infectious agent typically include the natural birth and death rates of a population. Also relevant to an

Received by the editors April 14, 2013 and, in revised form, April 22, 2013.
2000 *Mathematics Subject Classification.* 37Mxx, 92Bxx, 37Nxx, 65Yxx, 65Pxx.
This research was supported by NSERC Individual Discovery Grant.

infectious agent's dynamics is an incidence function, or a function that describes how infected and susceptible individuals contact.

There are various models used to describe the dynamics of infectious diseases, some of which are as follows [3, 5]:

- SIR, or Susceptible - Infected - Recovered. SIR models assume that susceptible people become infected, recover, and then remain immune to any further infection.
- SIRS, or Susceptible - Infected - Recovered - susceptible. SIRS models assume that after a person recovers, they become susceptible again after their immunity wears off.
- SEIR, or Susceptible - Exposed - Infected - Recovered. SEIR models assume that before a person enters an infected state where the disease is contagious, they first traverse a stage of being 'exposed' meaning they carry the infectious agent, but are not able to transmit it to others.

Some models assume that a recovered person will not exhibit any sort of immunity where other models incorporate a period of immunity after recovery. The duration of immunity can be treated as constant, or in more accurate models, treated as varying. The latter incorporates the notion of distributed delay in immunity duration into functions that govern re-susceptibility.

In this note, we consider an SIRS model, with constant immunity duration, subject to parameters for the birth and death rates of the population, transmission rate of the infectious agent, and recovery rate. We use a generalized incidence function in the model, but choose a specific one for the computation of numerical results. The main goal of this note is to perform bifurcation and sensitivity analysis via numerical simulations to discuss the role of the immunity duration on the disease transmission dynamics.

2. Mathematical Model

We assume that a small proportion of the population has become infected by some disease. The infected individuals interact with the susceptible individuals causing more people to move from the susceptible stage to the infected stage. Infected individuals then recover at a certain rate. They remain recovered and insusceptible for a certain time while their immunity persists. After some duration of immunity, however, they become susceptible and subject to potential infection again.

We further assume that people at all stages die at a natural death rate, thus all stages decrease accordingly. The susceptible population, however, is subject to population increase due to a flux of people into the system through natural birth. We also assume that the natural birth rate and natural death rate are equal so as to maintain a constant total population.

We define variables for the population densities of the three stages, susceptible, infected, and recovered: $S(t)$ - Susceptible, $I(t)$ - Infected, $R(t)$ - Recovered/Immune. We define the parameters that represent natural mortality rate, recovery rate, transmission rate, and immunity duration: m - Natural Mortality Rate, g - Recovery Rate, p - Transmission Rate, τ - Immunity Duration.

The model has been constructed in [2,4] in which susceptible individuals become infected at transmission rate p and in proportion to the susceptible population and the incidence function f(I(t)) of the infected population. The infected individuals recover into a stage of immunity at the recovery rate g. After some time τ, those

recovered become susceptible again as immunity wears off. The population at all stages suffers death at an equal natural death rate m, and that new births enter into the susceptible stage at the same rate m.

The model includes a group of delay differential equations that describe the rate of change of each of the three stages in terms of the other stages and parameters and incidence function described previously. The system of delay differential equations are provided by

$$\begin{aligned}\frac{dS}{dt} &= m - pf(I(t))S(t) - mS(t) + gI(t-\tau)e^{-m\tau},\\ \frac{dI}{dt} &= pf(I(t))S(t) - mI(t) - gI(t),\\ \frac{dR}{dt} &= gI(t) - gI(t-\tau)e^{-m\tau} - mR(t).\end{aligned}$$

Since the death rate and the birth rate are the same, the total population will remain constant. This can be obtained in the model by considering the sum of the three individual rates of change:

$$\frac{dS}{dt} + \frac{dI}{dt} + \frac{dR}{dt} = 0.$$

That is, the cumulative change in the population is zero. Integrating to obtain

$$S + I + R = constant = P.$$

The model has an internal steady state:

$$S^* = \frac{g+m}{p},$$

$$I^* = \frac{m(g+m) - mp}{p(ge^{-m\tau} - m - g)},$$

$$R^* = 1 - S^* - I^*.$$

3. Numerical Solutions

We now consider the qualitative behaviors of its solutions. To do so, we design programs to define, solve, and plot various solutions to the model. We develop Matlab programs to plot the solutions for $S(t)$, $I(t)$, and $R(t)$ over time.

We define a set of initial conditions and an incidence function as follows: initial susceptible population $S(0) = 0.99$, initial infected population $I(0) = 0.01$, initial recovered population $R(0) = 0$, and incidence function $F(I(t)) = I(t)$. These will be used throughout the paper unless otherwise stated. We choose values for the parameters m, g, and p, as follows: mortality rate $m = 0.15$, recovery rate $g = 5$, and transmission rate $p = 15$.

We numerically compute solutions for various immunity durations and plot them in Figures 1 and 2. For each value of τ we also compute the theoretical steady state to compare with the numerical results.

We observe that some solutions tend to a stable equilibrium, while others tend to a limit cycle. For both small and large values of τ, stable equilibria emerge, while for some intermediate values of τ, limit cycles emerge. We speculate that the system undergoes both forward and backward Hopf bifurcations at certain critical values of τ.

To more clearly see how the solutions undergo bifurcation, we design a program that plots numerous solutions on top of each other computed over some range of τ values, incremented slightly each time. Each solution is plotted in a slightly

$\tau = 0.0$

Stable Steady State

$S^* = 0.34$ $I^* = 0.36$ $R^* = 0.00$

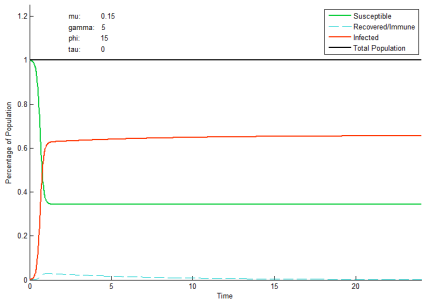

$\tau = 0.5$

Stable Steady State

$S^* = 0.34$ $I^* = 0.19$ $R^* = 0.46$

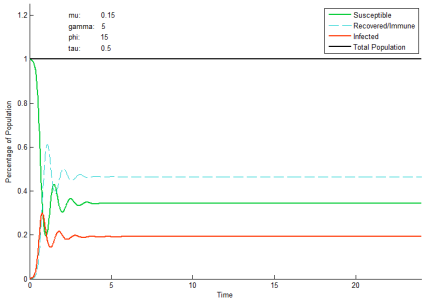

$\tau = 2.0$

Unstable Steady State

$S^* = 0.34$ $I^* = 0.07$ $R^* = 0.59$

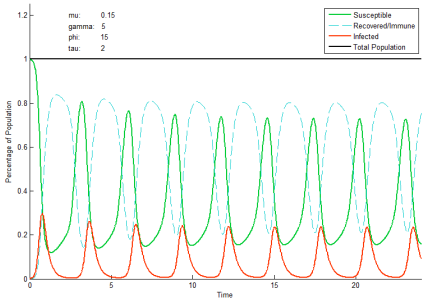

FIGURE 1. Solutions for different τ values.

$\tau = 4.0$

Unstable Steady State

$S^* = 0.34$ $I^* = 0.04$ $R^* = 0.62$

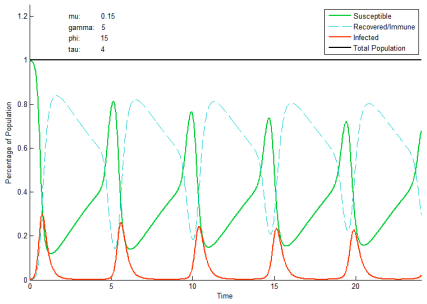

$\tau = 12$

Stable Steady State

$S^* = 0.34$ $I^* = 0.02$ $R^* = 0.63$

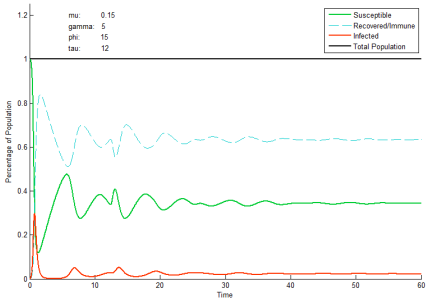

$\tau = 1000$

Stable Steady State

$S^* = 0.34$ $I^* = 0.02$ $R^* = 0.64$

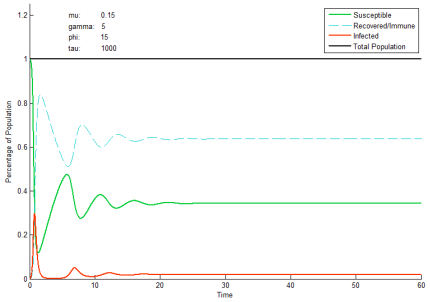

FIGURE 2. Solutions for different τ values (continued).

different color so as to show how they change as τ changes. We define the range for τ as: $\tau = 0.1$ to 2.1 in increments of 0.05. The result is plotted in Figure 3 which illustrates that each of the three stages gradually goes from exhibiting a steady state to a limit cycle.

4. Bifurcation and Sensitivity

At what exact point do the previously seen bifurcations occur? To determine this we first need to determine if any one specific solution exhibits a steady state or a limit cycle. We design a program called limitCycleFinder.m that takes one specific solution and assess whether a limit cycle exists. Detail on how this program works can be found in Appendix 1.

Next we design another program that can find the approximate value of τ at which the bifurcation occurs. This program attempts to find the value of τ that bifurcation occurs over some specified interval for τ. It first breaks the τ interval into a small number (specified in the program) of smaller subintervals and uses limitCycleFinder.m to determine over which sub interval the bifurcation occurs. It then repeats the process for the smaller interval until an interval is eventually found that is smaller than a tolerance incorporated into the function. It then takes the τ value at the midpoint of the final interval as an approximation of the bifurcation point.

Now we are able to find bifurcation points, and we are interested in qualitative assessment of bifurcation diagrams. We design a program to plot a three dimensional bifurcation diagram for a specific set of parameters and range of τ. It does so in the following manner:

(1) Computes solutions for specified number of τ values within a certain specified range.
(2) Eliminates the initial part of the solution trying to find a steady state or limit cycle by truncating the first half.
(3) Plots the solutions for $S(t)$ and $I(t)$ against the corresponding τ value in three dimensional space.

The result is plotted in Figure 4. From the first panel we observe gradually changing steady states for $S(t)$ and $I(t)$ for small values of τ, and then, after the bifurcation point, a limit cycle for $S(t)$ and $I(t)$ appears. The second panel suggests that the bifurcation point occurs somewhere near $\tau = 1.1$. Our program finds a more accurate approximate value of $\tau = 1.02$. It is worth noting that, to the naked eye, limit cycles do not seem to exist at $\tau = 1.02$. It takes the precision of numerical analysis to detect the smallest limit cycle invisible to the human eye.

So far we have considered the bifurcation point corresponding to one combination of parameters for m, g, and p. However, it is likely that bifurcation points will change as each of these parameters change. To check this, we calculate bifurcation points and plot corresponding bifurcation diagrams for combinations of parameters. Leaving p the same at $p = 15$, we show results for different values of m and g in Figure 5.

We see that, indeed, the bifurcation values change as m and g change, each exhibiting different bifurcation values. That is, the bifurcation value, τ^*, is a function of m and g. We denote this as $\tau(m, g)$. We can also consider how τ^* changes as a function of p and g. We denote this as $\tau(p, g)$.

In Figure 5 we have displayed the bifurcation values for each bifurcation diagram in varying colors. The color gradient on the right depicts how colors correspond to

Susceptible

(green for $\tau = 0.1$, blue for $\tau = 2.1$)

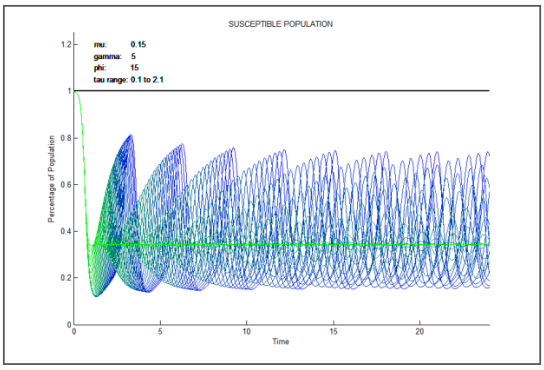

Infected

(red for $\tau = 0.1$, yellow for $\tau = 2.1$)

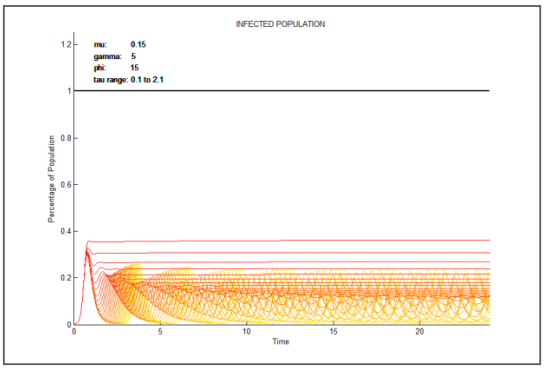

Recovered

(cyan for $\tau = 0.1$, magenta for $\tau = 2.1$)

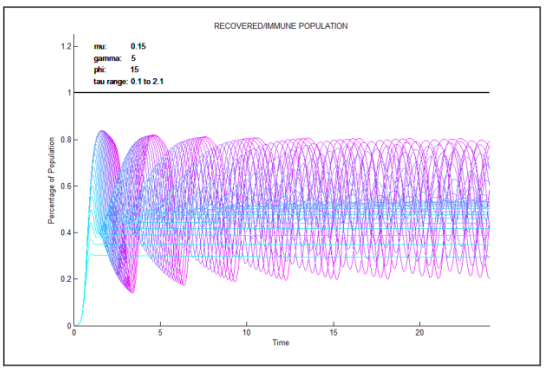

FIGURE 3. Transition of variables for varying τ.

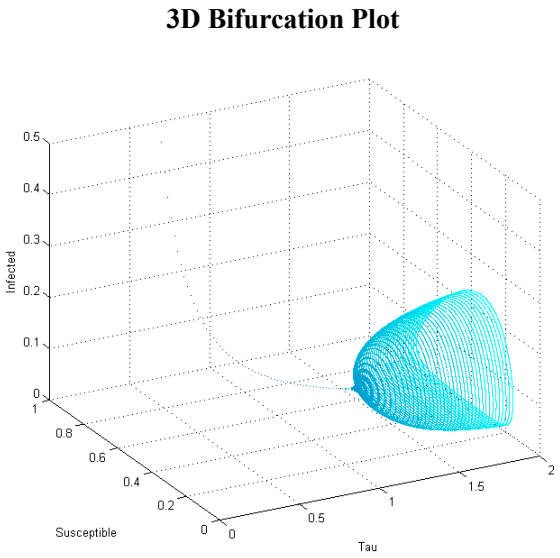

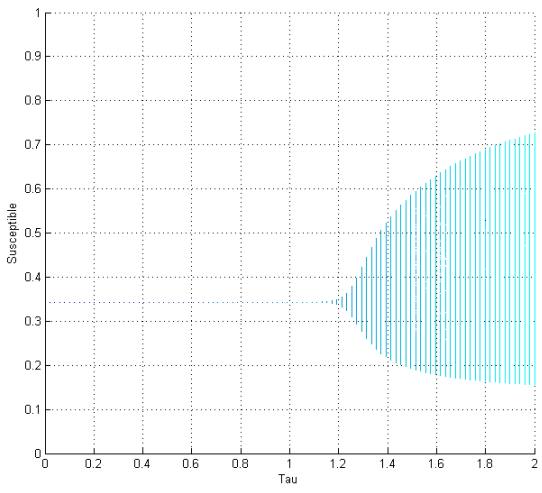

FIGURE 4. Bifurcation diagram of τ.

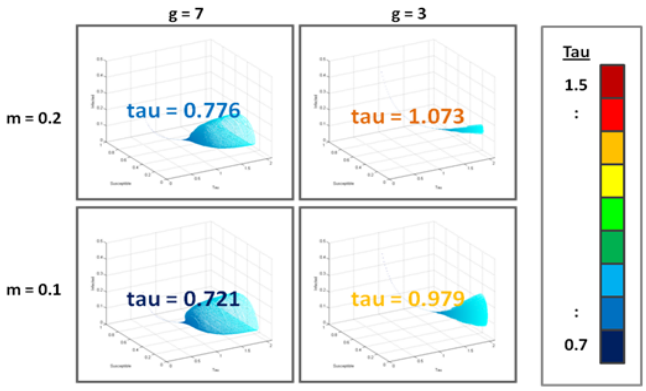

FIGURE 5. Bifurcation diagram of τ for different m and g values.

different bifurcation values. The colors simply represent the relative magnitude of the bifurcation values: blue for smallest and red for largest.

Next, we design a program to sequentially calculate bifurcation values over a two dimensional domain of parameters and then plot the resulting bifurcation values as a surface in three dimensional space. We do so for an (m, g) domain in the first panel of Figure 6, and for a (p, g) domain in the second panel of Figure 6.

The first panel of Figure 6 shows that τ^* increases as m increases, and decreases as g decreases for large g, but begins to increase again for smaller g. The second panel of Figure 6 shows that τ^* increases as p decreases, and only exhibits the behavior relative to g seen in the first panel for smaller p, that is, as g increases, τ^* first decreases and then begins to increase again. Moreover, in contrast with the first panel, the second panel shows that for small p, the bifurcation values for large g become large.

Having computed and plotted bifurcation values, another question arises: how sensitive is τ^* to small changes in each of the parameters? To answer this question, we perform sensitivity analysis.

The sensitivity of τ^* to each of our parameters is defined as

$$S_m^\tau = \frac{d\tau}{dm} \cdot \frac{m}{\tau},$$
$$S_g^\tau = \frac{d\tau}{dg} \cdot \frac{g}{\tau},$$
$$S_p^\tau = \frac{d\tau}{dp} \cdot \frac{p}{\tau}.$$

Since our solution surface for τ^* does not have an explicit representation, we must develop a numerical scheme to compute the sensitivities. We use a five point numerical differentiation method for the derivatives, discretizing the former continuous equations as follows:

$$S_{m_i}^{\tau_i} = \frac{\tau_{i+2} - 8\tau_{i+1} + 8\tau_{i-1} - \tau_{i-2}}{12h} \cdot \frac{m_i}{\tau_i},$$
$$S_g^{\tau_i} = \frac{\tau_{i+2} - 8\tau_{i+1} + 8\tau_{i-1} - \tau_{i-2}}{12h} \cdot \frac{g_i}{\tau_i},$$

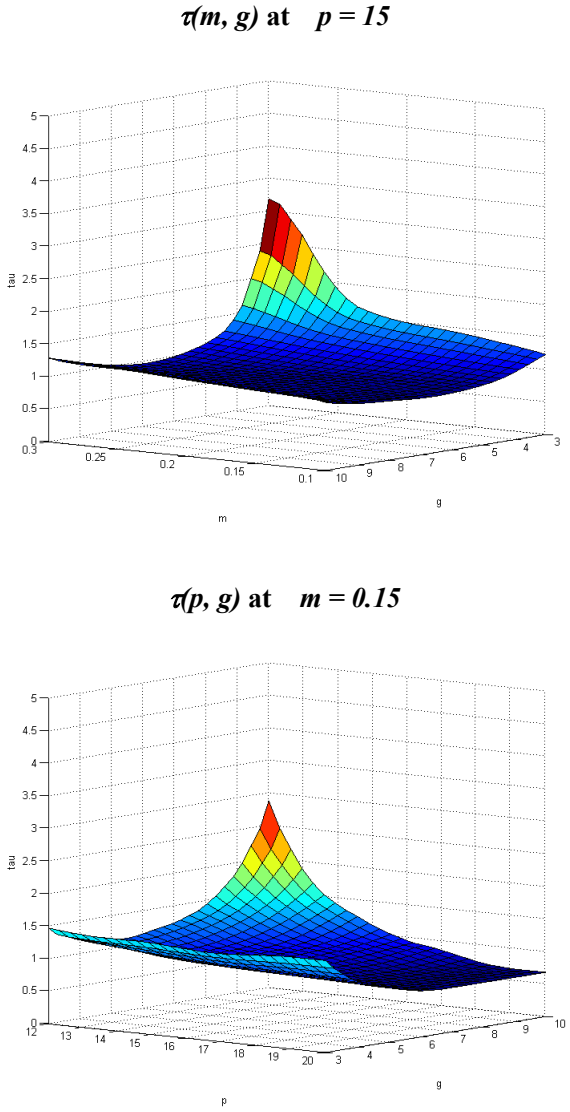

FIGURE 6. Sample bifurcation surfaces.

$$S_{p_i}^{\tau_i} = \frac{\tau_{i+2} - 8\tau_{i+1} + 8\tau_{i-1} - \tau_{i-2}}{12h} \cdot \frac{p_i}{\tau_i},$$

where i is the index in the direction of the parameter we are calculating sensitivity relative to.

For sensitivities at both the boundaries and index directly adjacent to the boundaries we use two and three point numerical differentiation schemes respectively. For example, in computing S_m^τ at $i = 0$ we use the two point method:

$$\frac{d\tau}{dm} = \frac{\tau_{i+1} - \tau_i}{\Delta m}$$

to compute the derivative. And at $i = 1$ we use the three point method:

$$\frac{d\tau}{dm} = \frac{\tau_{i+1} - \tau_{i-1}}{2\Delta m}.$$

We do the same approximation at the other boundary, and the analogous procedure for S_g^τ and S_p^τ.

We first consider the sensitivity of τ^* to the change in g. The first panel of Figures 7 shows the corresponding sensitivity surface to the first panel of Figure 6, $\tau(m, g)$, and the second panel of Figure 7 shows a similar surface as the second panel of Figure 6, $\tau(p, g)$. We observe that τ^* becomes more sensitive to g as g increases in both cases. The sensitivity of τ^* to g stays relatively flat as m changes, except for large m when g is either large or small. The sensitivity of τ^* to p increases faster as g increases.

Next we consider the sensitivity of τ^* to the change in m. The first panel of Figure 8 shows the corresponding sensitivity surface to the first panel of Figure 6, $\tau(m, g)$. We observe that the sensitivity of τ^* to m increases quicker as m and g increase together but stays relatively flat otherwise. The sensitivity in this case is positive, meaning that τ^* changes in the same direction as m.

Finally we consider the sensitivity of τ^* to the change in p. The second panel of Figure 8 shows the corresponding sensitivity surfaces to the second panel of Figure 6, $\tau(p, g)$. We observe that the sensitivity of τ^* to p decreases quicker as both p decreases and g increases. Furthermore, the sensitivity in this case is negative, indicating that τ^* changes in the opposite direction of the direction of the change in p. For example, an increase in p will result in a decrease in τ^*.

5. Backward Bifurcations and Period of Limit Cycles

So far we have only considered forward bifurcations. The question of what happens to our solutions after this first bifurcation has occurred, however, now arises. Will the exhibited limit cycle then undergo a backward bifurcation and become a stable equilibrium again? We show that backward bifurcations do exist in Figure 9, similar to Figure 4, but here for τ from 1 to 12.

Clearly, τ does undergo a backward bifurcation as the limit cycle disappears and becomes stable again. Figure 9 shows a backward bifurcation occurring near $\tau = 5$. This figure also reveals an interesting observation between $\tau = 6$ and $\tau = 10$. It is unclear at this point if it is the emergence of another limit cycle and two more bifurcations, or simply the result of our programs plotting the bifurcation diagrams for not sufficiently long time on this interval.

We have considered the existence of limit cycles, but until now, have given no attention to their periods. For certain values of τ, limit cycles emerge, but what can we say of the limit cycles themselves? Do their periods change as τ changes?

We design a program to compute the period of a given solution. The program takes a solution vector and a domain vector as inputs and, after computing the period of the solution's limit cycle (if it exists), outputs a numerical value for it.

We then design a program to plot the period of solutions for a specific set of parameters (m, g, p) as a function of τ. We show various plots of the period as a function of τ in Figure 10.

Figure 10 shows that for small values of τ no limit cycles exist (depicted on the plots as periods of 0). After bifurcation occurs we see the period of the limit cycle plotted immediately to the right of the bifurcation point. Then, as τ increases further, we see the period of the limit cycle increases in all cases. Finally, in the

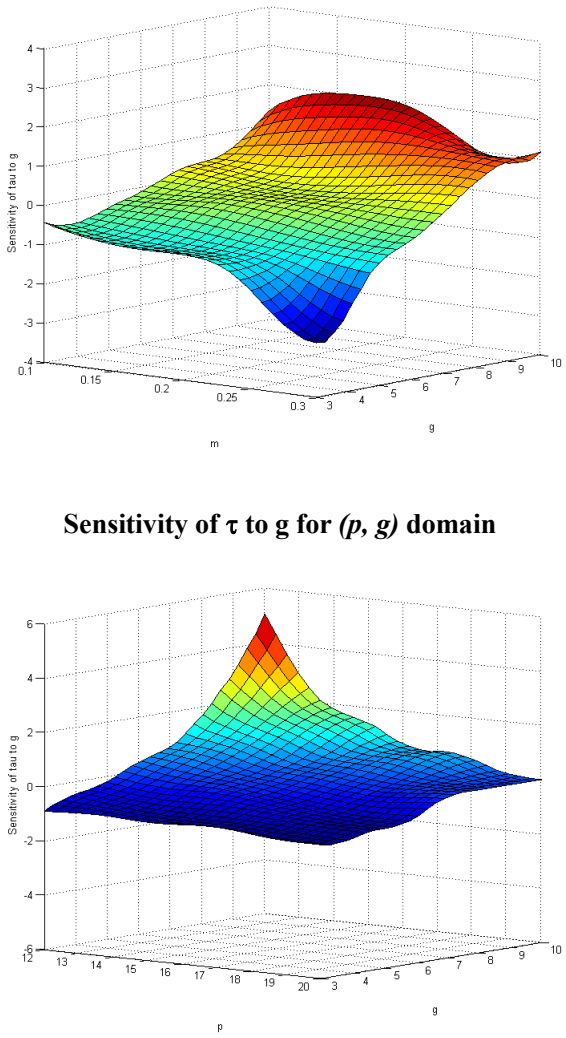

FIGURE 7. Sensitivity analysis.

plots where the domain for τ is large enough, we see the period drops to zero again, indicating the disappearance of the limit cycle.

We have plotted the period verses τ for a specific set of parameter values for m, g, and p. How does the period change with respect to changes in the three parameters?

We design a program to calculate and plot the period of the limit cycle as a function of both τ and one of the parameters m, g, or p. The program plots an array of "dots" in three dimensional space with the colors of each "dot" dependent

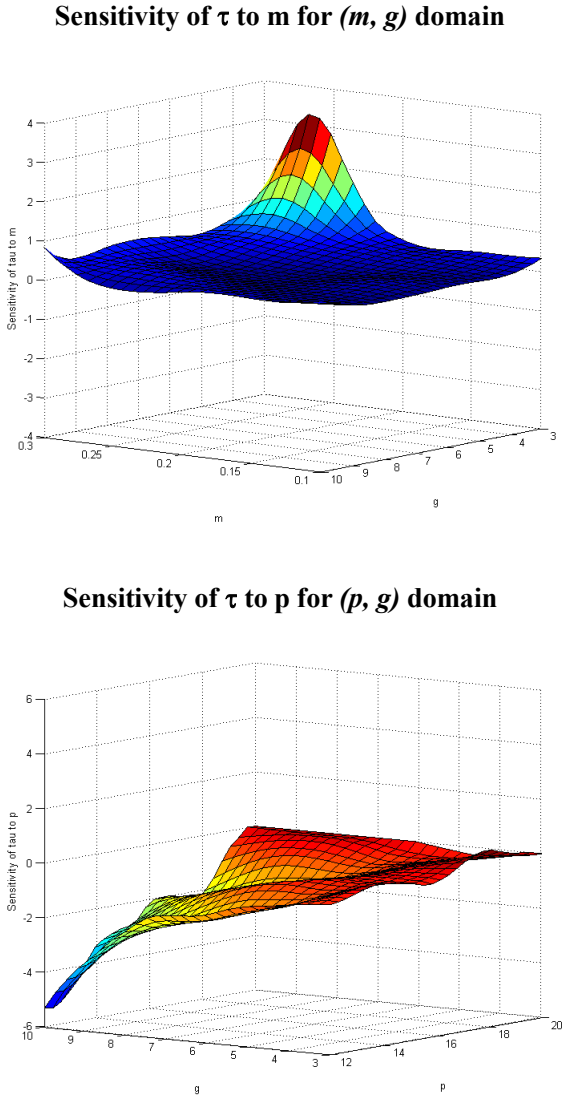

FIGURE 8. Sensitivity analysis (continued).

on the value of the period for that solution: the lighter the color, the higher the period. We show the results in Figures 11,12,13.

The first panel of Figure 11 shows the domain for which limit cycles exist (the lighter green). The three dimensional plot in the second panel shows the corresponding period of the limit cycle. The period increases as τ increases. To evaluate how the period changes as g changes, our attention is drawn to the third panel. We

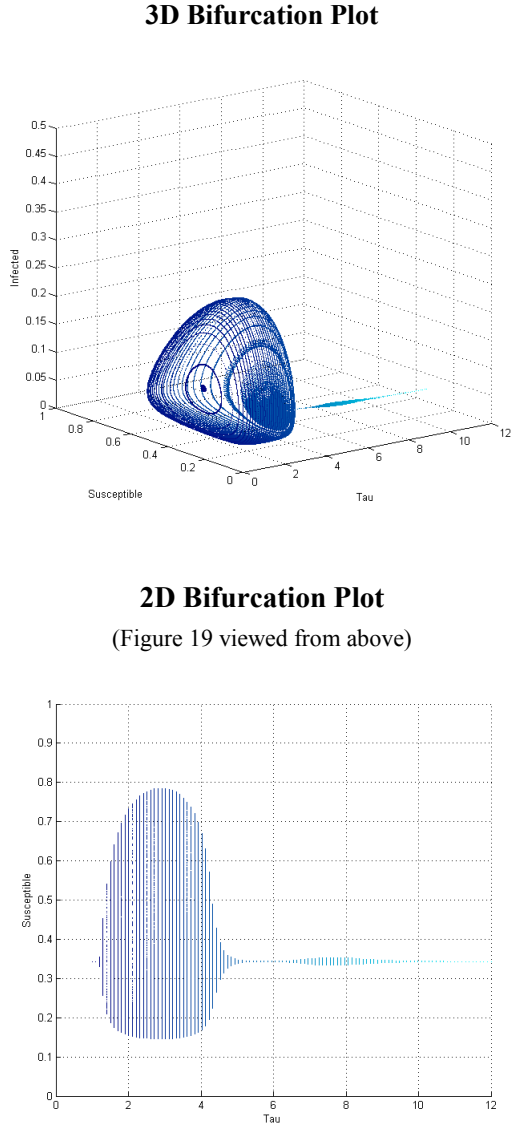

FIGURE 9. Backward bifurcation.

observe that the period also changes as g changes, but not as drastically. Indeed, τ is the more sensitive parameter.

We now produce similar plots for the period as a function of τ and m and p, respectively, in Figures 12 and 13. Again we see that the period changes as τ and both m and p change and that the period is most sensitive to the change in τ.

6. Concluding Remarks

Throughout this note we have considered a specific case of an SIRS model with a constant delay corresponding to immunity duration. We showed how different

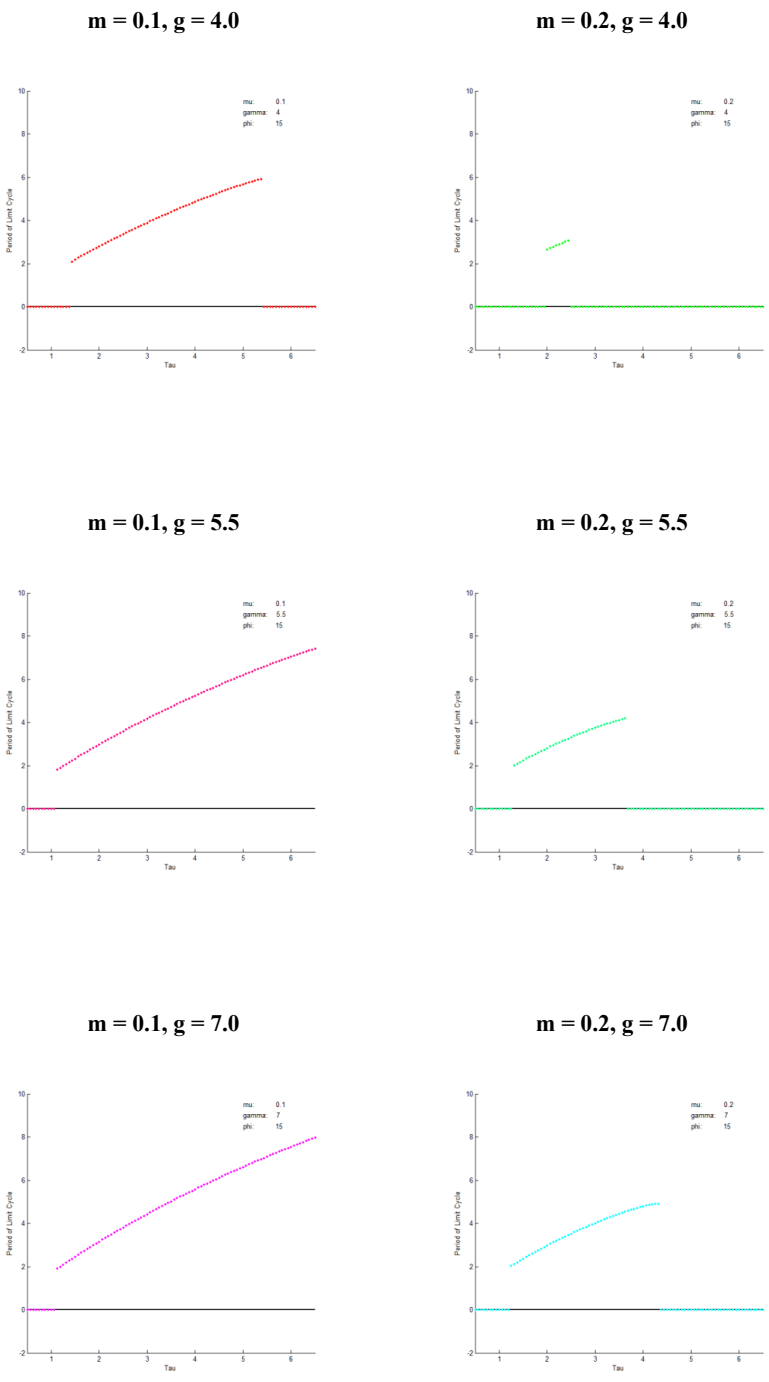

FIGURE 10. Bifurcation diagrams for period of the limit cycle.

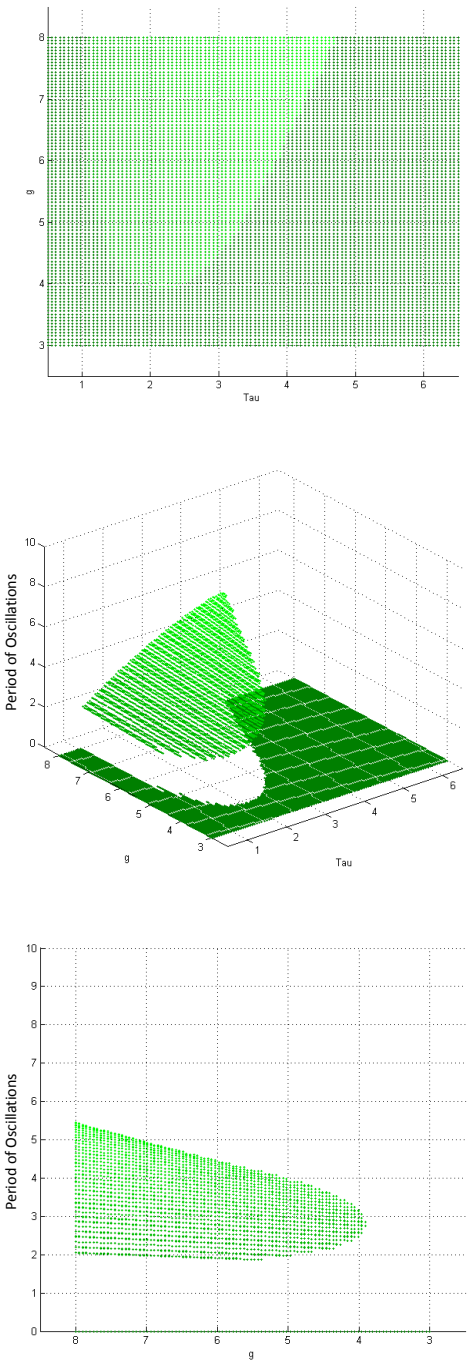

FIGURE 11. Two dimensional bifurcation diagrams of g and τ for period of the limit cycle.

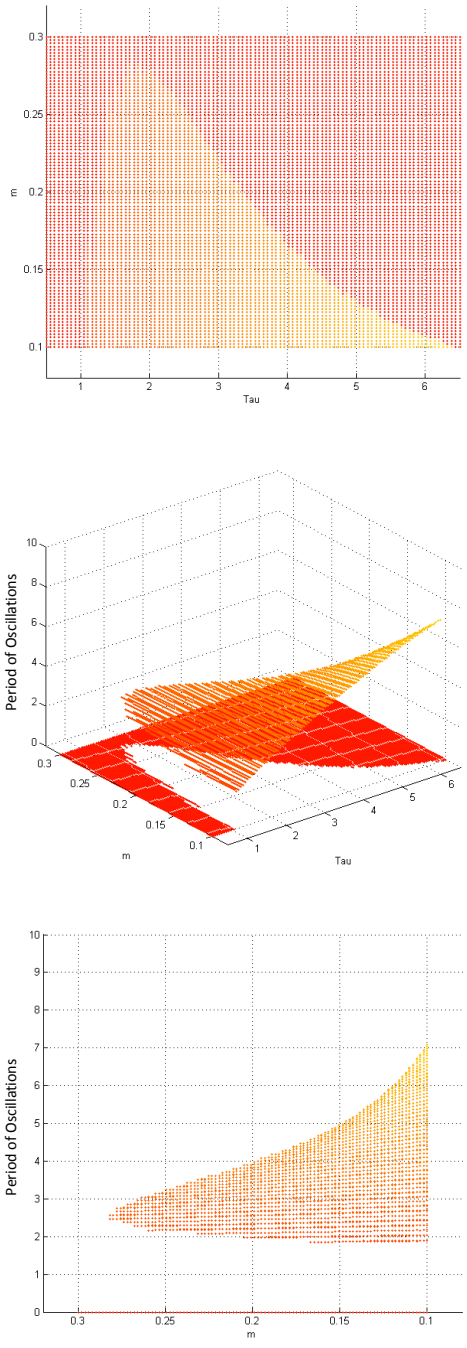

FIGURE 12. Two dimensional bifurcation diagrams of m and τ for period of the limit cycle.

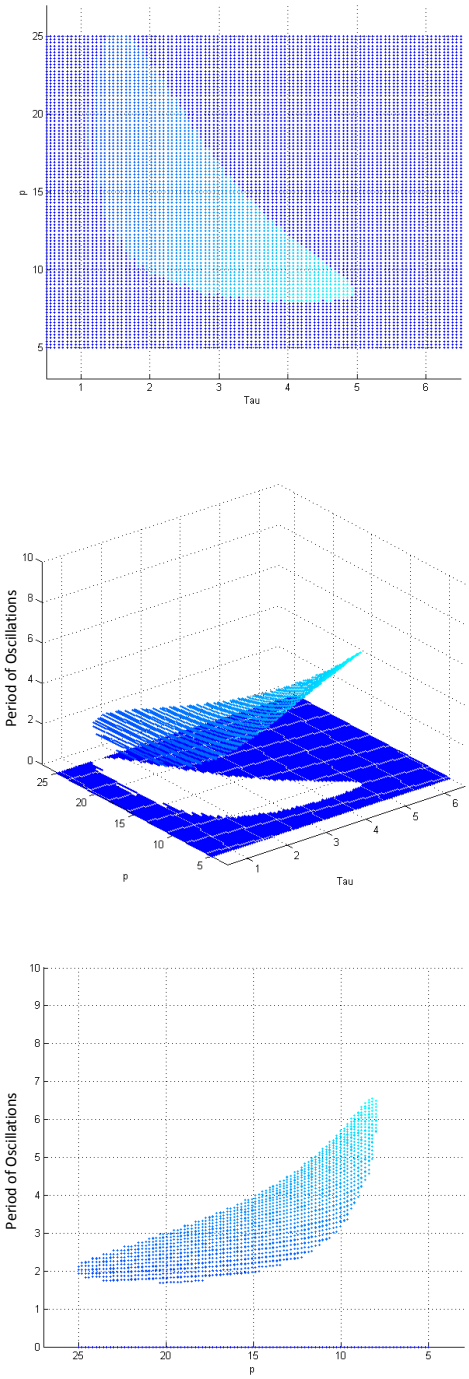

FIGURE 13. Two dimensional bifurcation diagrams of p and τ for period of the limit cycle.

combinations of parameter values for natural birth/death rate, transmission rate, and recovery rate, alongside different values for immunity duration, can result in either a stable equilibrium or a limit cycle. Moreover, we were able to show how the forward bifurcation value varies with changes in the parameters. We numerically computed bifurcation values for two arrays of parameter combinations and plotted them as bifurcation surfaces.

We then computed the sensitivities of the bifurcation values relative to each of their parameter arguments and plotted them as surfaces as well. This numerical sensitivity analysis showed us that the bifurcation values are especially sensitive to changes in certain parameters in certain regions of the corresponding parameter space. Considering the parameter space $(m, g, p) = [0.1, 0.3] \times [3, 10] \times [12, 20]$, the regions most noteworthy are

Sensitivity of τ to	**Parameter Space**	**Sensitivity**	**Sensitive Region**
m	(m, g)	positive	m large, g small
g	(m, g)	negative	m large, g small
g	(m, g)	positive	g large
g	(p, g)	positive	p small, g large
p	(p, g)	negative	p small, g large

In other words, the points at which outbreaks emerge are most sensitive to the birth/death rate when the birth/death rate is large, and the recovery rate is small (positive sensitivity).

The points at which outbreaks emerge are most sensitive to the recovery rate when

(1) The birth/death rate is large, and the recovery rate is small (negative sensitivity).
(2) The recovery rate is large (positive sensitivity).
(3) The recovery rate is large, and the transmission rate is small (positive sensitivity).

The points at which outbreaks emerge are most sensitive to the transmission rate when the recovery rate is large, and the transmission rate is small (negative sensitivity).

We then shifted our attention to the period of the limit cycle itself and how it changes with changes in the parameters and with the change in immunity duration. We found that the period would change slightly with changes in the parameters: period would increase with the increase in birth/death rate, increase with the increase in recovery rate, and decrease with the increase in transmission rate. Period would, however, change much more drastically with the change in immunity duration. In all cases, the period of all outbreaks would increase by as much as two or three times as the duration of immunity increases.

We have analyzed one specific model, with a specific incidence function, over a range of parameter values. One may wonder to what gain has such work been done? Specific infectious agents command the use of specific models, with specific parameter domains. Having shown in detail how our numerical analysis can provide insight into the behavior of a model's solutions and their sensitivity to the parameters involved, it remains only a small step to repeat such analysis for a specific model corresponding to a specific infectious agent when times deem necessary. As an example, we plot bifurcation diagrams for different incidence functions in Appendix 2.

Our analysis can be applied to any similar SIR or SIRS model, with or without a constant delay for immunity duration. Moreover, since we designed programs from scratch, modifying our programs for models that incorporate distributed delay will only require minimal efforts as well.

7. Appendices

Appendix 1 - limitCycleFinder.m

One of the more challenging tasks was designing a program to determine if a limit cycle exists in a specific solution. Doing so analytically is possible when the model is simple. Doing so by qualitative visual inspection is possible when the limit cycle is large enough. Both accounts fail for the purpose of this note, specifically, in respect to computing bifurcation points.

To determine a bifurcation point, we need to determine the first value of τ for which a steady state starts to oscillate in the smallest amount. Doing so analytically fails because of the complexity of the model; doing so visually is subject to intolerable error in both a person's eye and a computer's discrete display of pixels. A limit cycle of minute amplitude would remain undetectable. Moreover, at times we need to assess thousands or even millions of solutions, which, of course, would be impossible in the absence of automation.

How does limitCycleFinder.m work? An individual solution with or without a limit cycle would typically look something like the two graphs in Figure 14.

As can be seen, each solution has a series of maximums and minimums. Each max or min can be represented by a point $(t, y(t))$. limitCycleFinder.m assumes that the path traversed by consecutive maximums and minimums is of the form:

$$y(t) = ae^{bt} + c.$$

We have yet to prove this assumption and such endeavor may be topic of further work. However, in applications, the assumption proves useful as shown throughout this note.

Using vectors of points for the sequences of maximums and minimums, the script first optimizes the parameters a, b, and c to best fit exponential curves of the above form to each of the two sets of points. The results typically look something like the two graphs in Figure 15.

The green and the red points are the maximums and minimums determined by the program. The green and red lines are the exponential curves fit to these points. We have two functions for the two exponential curves. For the maximum:

$$y_1(t) = a_1e^{b_1t} + c_1$$

and for the minimum:

$$y_2(t) = a_2e^{b_2t} + c_2.$$

Since both b_1 and b_2 are negative, it is clear that

$$\lim_{t\to\infty} y_1(t) = c_1$$

and

$$\lim_{t\to\infty} y_2(t) = c_2.$$

That is, y_1 and y_2 are asymptotic to c_1 and c_2, where c_1 and c_2 approximate the maximum and minimum amplitude of the limit cycle. If a limit cycle exists, its

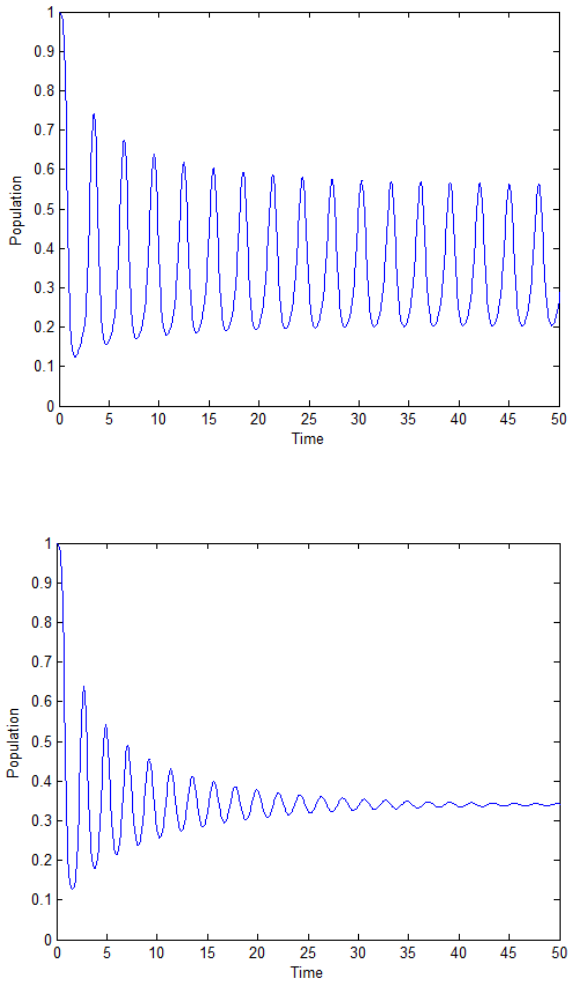

FIGURE 14. Sample solutions with or without a limit cycle.

amplitude must be greater than zero. Thus, $c_1 - c_2 > 0$. Likewise, it a limit cycle does not exist, we have $c_1 = c_2$.

However, since the best fitting curves quite likely yield some measure of error, we allow for a small tolerance ε. In other words, the program draws conclusions according to the following: If $c_1 - c_2 > \varepsilon$, then a limit cycle exists. And if $c_1 - c_2 < \varepsilon$, then a limit cycle does not exist.

Appendix 2 - Different Incidence Functions

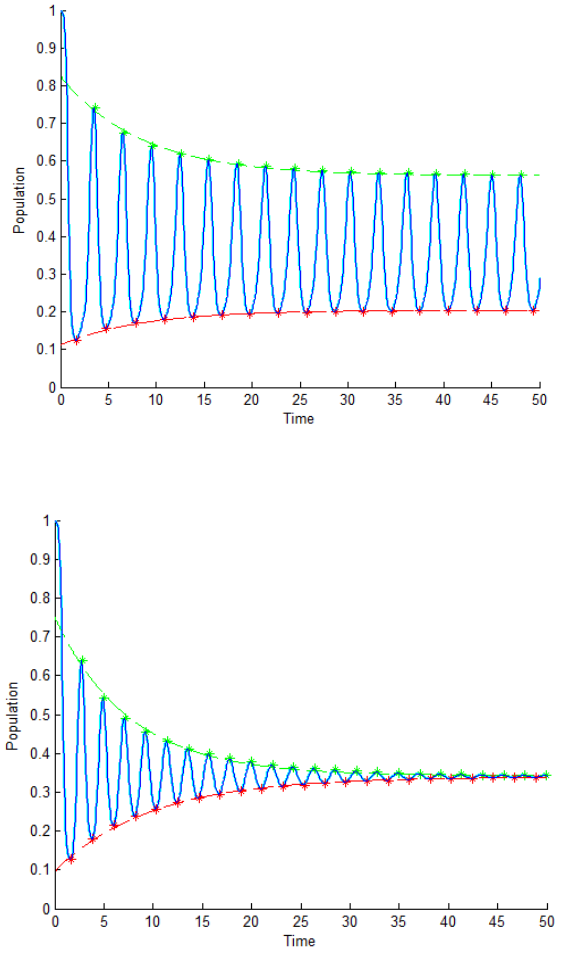

FIGURE 15. Illustration of determining max and min.

In this note, we have used a simple incidence function $f(I(t)) = I(t)$. Although not particularly relevant to the specific analysis done here, the use of different incidence functions does arise in the use of models for specific diseases.

Using the same specific parameter values: $m = 0.15, p = 15, g = 5$ as in the earlier part of the paper, we briefly consider how bifurcation diagrams change as a result of different incidence functions. Four specific bifurcation diagrams for different incidence functions are plotted in Figure 16.

We can observe that the behavior of the model respective to differing incidence functions changes. The amplitude of the emergent limit cycles changes as well as their bifurcation points. Furthermore, in two of the previous cases, bifurcations, and thus limit cycles, cease to exist at all.

We could, of course, work through the same analysis, running the same simulations as in the main part of the paper, for each incidence function, but we leave

$$f(I) = I$$

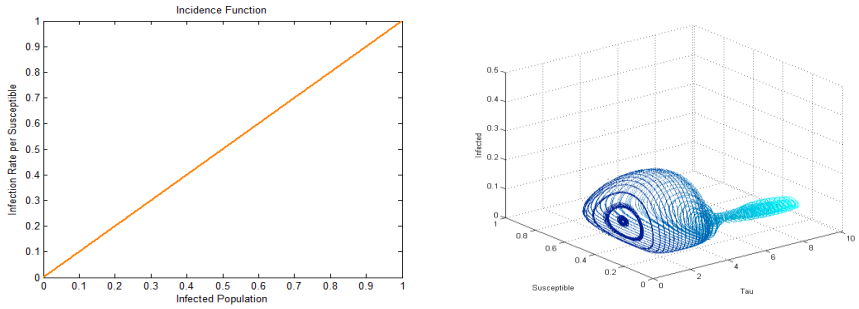

$$f(I) = \frac{I}{1+I}$$

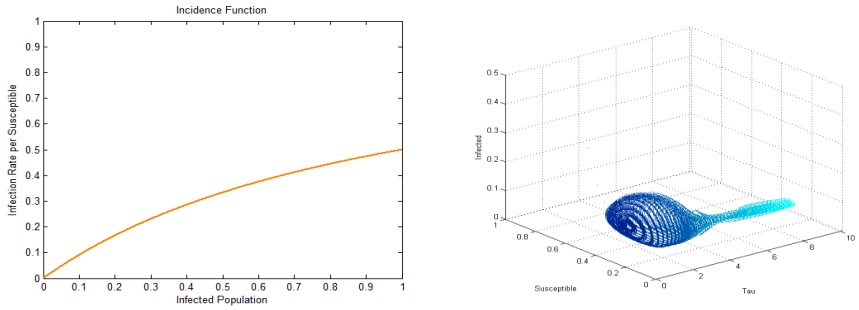

$$f(I) = \frac{I}{0.1+I}$$

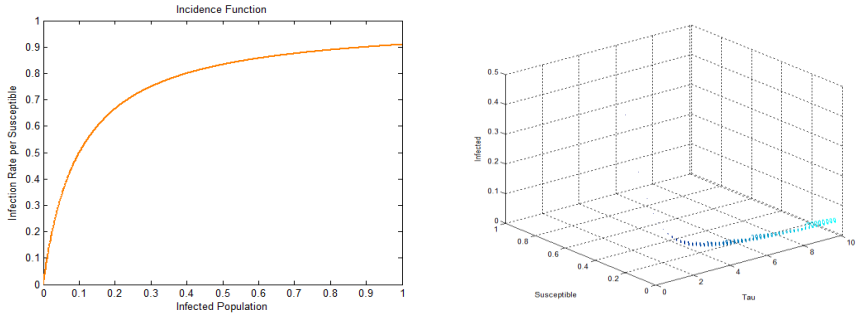

$$f(I) = e^{-\pi I}$$

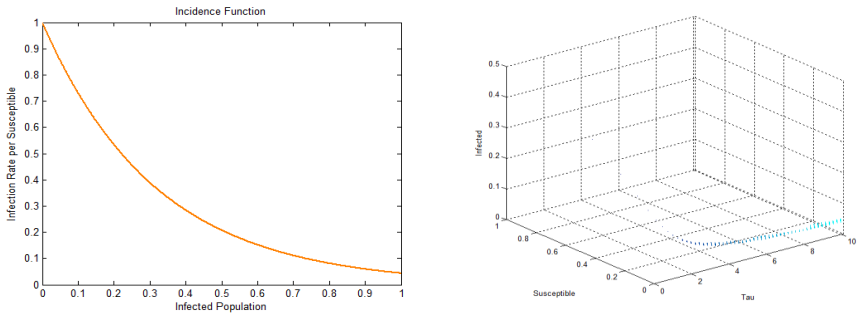

FIGURE 16. Bifurcation diagrams for different incidence functions.

such analysis to the time when a specific model with a specific incidence function calls for it.

References

[1] Anderson, R.M. and May, R.M., Infectious Diseases of Humans: Dynamics and Control, Oxford University Press, New York, 1992.
[2] Blyuss, K.B. and Kyrychko, Y.N., Stability and Bifurcations in an Epidemic Model with Varying Immunity Period, Bulletin of Mathematical Biology, Vol 72, 490-505, 2010.
[3] Keeling, M.J. and Rohani, R., Modeling Infectious Diseases in Humans and Animals, Princeton University Press, Princeton, NJ, 2008.
[4] Kyrychko, Y.N. and Blyuss, K.B., Global properties of a delayed SIR model with temporary immunity and nonlinear incidence rate. Nonlinear Anal. RWA, Vol 6, 495-507, 2005.
[5] Pollicott, M., Wang, H., and Weiss, H., Extracting the time-dependent transmission rate from infection data via solution of an inverse ODE problem, Journal of Biological Dynamics, Vol. 6, 509-523, 2012.

Department of Mathematical and Statistical Sciences, University of Alberta, Edmonton, AB T6G 2G1, Canada

E-mail: hao8@ualberta.ca